

## LETTER

# Parallel selective pressures drive convergent diversification of phenotypes in pythons and boas

Damien Esquerré\* and J. Scott Keogh

Division of Evolution, Ecology and Genetics, Research School of Biology, The Australian National University, Canberra, ACT 0200, Australia

\*Correspondence: E-mail: damien.esquerre@anu.edu.au

### Abstract

Pythons and boas are globally distributed and distantly related radiations with remarkable phenotypic and ecological diversity. We tested whether pythons, boas and their relatives have evolved convergent phenotypes when they display similar ecology. We collected geometric morphometric data on head shape for 1073 specimens representing over 80% of species. We show that these two groups display strong and widespread convergence when they occupy equivalent ecological niches and that the history of phenotypic evolution strongly matches the history of ecological diversification, suggesting that both processes are strongly coupled. These results are consistent with replicated adaptive radiation in both groups. We argue that strong selective pressures related to habitat-use have driven this convergence. Pythons and boas provide a new model system for the study of macro-evolutionary patterns of morphological and ecological evolution and they do so at a deeper level of divergence and global scale than any well-established adaptive radiation model systems.

### Keywords

Adaptive radiation, ecomorphology, henophidia, snakes.

Ecology Letters (2016) 19: 800–809

## INTRODUCTION

Adaptive radiation, when descendants from a common ancestor rapidly fill a variety of ecological niches, is one of the main drivers of ecological and morphological diversity (Schluter 2000; Gavrillets & Losos 2009). Adaptive radiations often have revealed within them repeated evolution of similar solutions to similar problems (i.e. convergent evolution) (McGhee 2011). But more rarely, two distantly related clades or adaptive radiations can respond similar to the same set of selective pressures operating in different places, resulting in the independent evolution of the same phenotypes adapted to the same ecological niche (Bossuyt & Milinkovitch 2000; Moen *et al.* 2015). If a trait exhibits an association with a particular environment or ecological factor that has evolved repeatedly in different species across different lineages, it is likely to be an adaptation to that environment (Simpson 1953; Harmon *et al.* 2005; Losos 2011). This is the basis of comparative analyses that seek to identify potential adaptations.

Most researchers have focused on convergence within clades of closely related species that inhabit islands or lakes in the same general region [e.g. Caribbean anole lizards (Mahler *et al.* 2013), African Great Lake cichlid fishes (Muschick *et al.* 2012)]. However, this phenomenon also can occur at much deeper phylogenetic levels between major radiations in more disparate taxa (Donley *et al.* 2004; Melville *et al.* 2006). Nevertheless, this is rare and often incomplete because historical contingencies and divergence in some phenotypic axes can prevent distantly related taxa from responding identically to natural selection. Moreover, if many phenotypic solutions exist for a functional problem then convergence is not necessarily the outcome (Wainwright *et al.* 2005). Therefore, replicated adaptive radiations, rather than just convergence within a clade, are even more rare and proposed cases require further

examination (Losos 2010). Such cases often are based on general similarities in appearance (e.g. numbats and anteaters or wolves and thylacines in the comparison between the radiations of placental and marsupial mammals), rather than rigorous quantitative similarities. Testing hypotheses about convergent evolution driven by natural selection is vastly improved if we can apply tests to phylogenetically distant adaptive radiations that each have diversified into different continents and display diverse ecological life-styles or ‘guilds’ (Harvey & Pagel 1991).

The pythons and boas are two species-rich and phenotypically and ecologically diverse snake radiations. Each radiation comprises species that are arboreal, semi-arboreal, terrestrial, semi-aquatic and semi-fossorial (Fig. 1), and they also show great diversity in adult body size, ranging from pygmies to the largest snakes on earth such as the reticulated python (*Malayopython reticulatus* (Schneider, 1801)) and green anaconda boa (*Eunectes murinus* (Linnaeus, 1758)). Although once lumped in the same family, pythons and boas are not each other's closest relatives. They are each more closely related to other small to medium-sized cryptozoic or burrowing snake lineages (Reynolds *et al.* 2014). Together they belong to a group called the Henophidia and last shared a common ancestor in the mid-late Cretaceous, 63–96 Mya (Pyron & Burbrink 2014; Hsiang *et al.* 2015; Streicher & Wiens 2016; Zheng & Wiens 2016). Pythons are exclusively an Old World radiation with 44 species distributed through Africa, Asia, and, most notably diverse, in the Australo-Papuan region. Boas comprise 58 species, and are widely distributed around the world. They are especially diverse in subtropical and tropical areas, but are absent in Australia. We use a phylogenetic framework to test whether there is convergent evolution in head shape driven by parallel adaptation to similar ecological niches between the distantly related pythons and boas. We acknowledge that

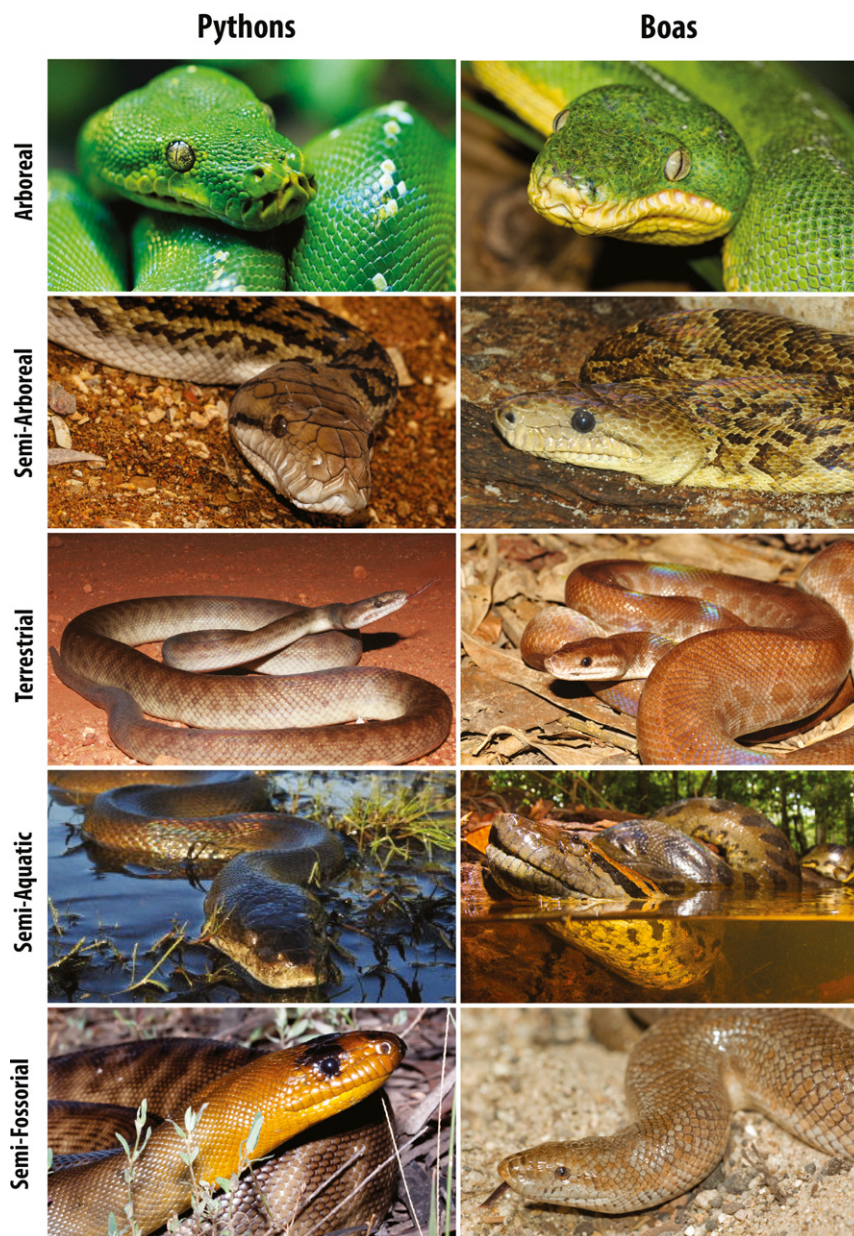


**Figure 1** Convergent ecological guilds in pythons and boas. Examples of pythons and boas that display a similar micro-habitat or guild and look phenotypically similar. Species pairs from top to bottom and left to right along with the author of the photograph are as follows. Arboreal: *Morelia viridis* (John Rummel) and *Corallus caninus* (Pedro Bernardo). Semi-arboreal: *Similia kinghorni* (Kieran Palmer) and *Chilabothrus angulifer* (Milan Kořínek). Terrestrial: *Antaresia childreni* (Dan Lynch) and *Epicrates maurus* (Esteban Alzate). Semiaquatic: *Liasis mackloti* (George Cruiser) and *Eunectes murinus* (Marcio Lisa/Txai Studios). Semi-fossorial: *Aspidites ramsayi* (Steve Wilson) and *Lichanura trivirgata* (Pedro Bernardo).

there is a conceptual debate on the terminology of ‘convergence’ and ‘parallelism’ (Arendt & Reznick 2008). Here, we will refer to convergence as simply the independent evolution of the same or similar phenotypes.

## MATERIALS AND METHODS

### Specimens and phenotypic data acquisition

We examined 1073 specimens from 94 taxa (including some subspecies) of henophidian snakes (Table S1). We were able to include 82% of the Booidea species ( $n = 45$ ) and 77% of

the Pythonidae ( $n = 34$ ) and measured an average of 11.4 specimens per species (range = 1–59). See Supplementary Information for taxonomic comments. We also included species from most of the other henophidian lineages (except Xenophiidae and Anomochilidae): Loxocemidae, Xenopeltidae, Cylindrophiiidae, Uropeltidae, Tropidophiidae, Aniliidae and Bolyeriidae (see Table S1). Specimens were measured in the following collections: the Queensland Museum, the Museum and Art Gallery of the Northern Territory, the South Australian Museum, the Western Australian Museum, the Australian Museum, the California Academy of Sciences, the University of Texas at Arlington, the American Museum



of Natural History and the Museum of Comparative Zoology. We restricted our data collection to adults with well-preserved heads, and for each species we used the largest specimens available. For each specimen we took a photograph of the dorsal surface of the head with a Canon 7D camera and a Canon macro 100 mm lens with a Canon Twin-Lite macro flash (Canon Inc., Tokyo, Japan) mounted on a tripod and shooting directly from above. We placed a scale-bar next to each specimen to enable scaling of the landmark data (see below).

### Geometric morphometrics

We assessed head shape using landmark-based geometric morphometrics (Zelditch *et al.* 2012). We digitised 9 landmarks and 26 semi-landmarks that accurately describe head shape on each photograph (Fig. S1) using *tpsDig* 2.17 (Rohlf 2015). We slid the semi-landmarks using the bending energy method in *tpsRelw* (Rohlf 2015) which were treated as homologous landmarks in the following analyses. Shape information was extracted with a Procrustes superimposition which removes the effect of location, orientation and scale from the data (Rohlf & Slice 1990) using *MorphoJ* 1.06 (Klingenberg 2011), and taking into account object symmetry (Klingenberg *et al.* 2002). To remove any allometric effects on shape we performed a multivariate pooled-within-genus regression of the symmetric component of shape on log-transformed centroid size, with a permutation test of 10,000 iterations to test against the null hypothesis of independence. Centroid size is measured as the square root of the sum of the squared distance of every landmark to the centroid or 'centre' of the landmark configuration, and is therefore a measure of the size of each specimen. Size was significantly related to shape, accounting for 8.01% of the variation ( $P < 0.0001$ ), therefore, for all subsequent analyses we used the regression residuals. To visualise shape variation in morphological space and reduce the dimensionality of the data to a few orthogonal variables, we performed a Principal Components Analysis (PCA). While there are some analytical challenges in using PCA to evaluate complex multivariate data in an evolutionary context, especially the 'sorting' principal components by different models of evolution (Uyeda *et al.* 2015), it is the best available approach for our purposes (e.g. Moen *et al.* 2015).

### Ecological and phylogenetic information

After a thorough literature review, we used 190 published sources (Table S1) to allocate each taxon to one of six ecological guilds: arboreal, semi-arboreal, terrestrial, semi-aquatic, semi-fossorial and fossorial. These guilds are defined by the main micro-habitat that a species uses when active or foraging. The semi-arboreal, semi-fossorial and semi-aquatic categories simply mean that these species also often forage actively on the ground. See Supplementary Information for a description of the main features and composition of each guild.

We used an explicitly phylogenetic approach to our analyses, including both phylogenetic comparative methods and phylogenetic visualisation of our geometric morphometric data. For both we used the recently published well resolved

phylogeny of henophidians (Reynolds *et al.* 2014). We converted the tree to ultrametric using a smoothing parameter  $\lambda = 0$  and pruned the tree to match the taxa in our dataset. To choose our  $\lambda$  we tested the fit of different values and extracted the penalised log likelihood. We found that the best fit was obtained with  $\lambda = 0$ . These procedures were done using the package *ape* (Paradis *et al.* 2004) for R. All analyses using R packages were performed with R version 3.2 (R Development Core Team 2015).

### Phylomorphospace reconstruction

To visualise the phylomorphospace we mapped the principal component scores on to the phylogeny using square change parsimony reconstruction of ancestral nodes (Maddison 1991) as implemented in *MorphoJ* (Klingenberg & Gidaszewski 2010). This approach provides an intuitive and visual way to examine the history and patterns of morphological evolution in a phylogenetic context (Sidlauskas 2008).

### Phenotypic convergent regimes and ancestral state reconstruction

To identify rate shifts and convergence of phenotypic optima on the tree we used a recently developed method called SURFACE (Ingram & Mahler 2013; Mahler & Ingram 2014) implemented in R. The method finds cases of phenotypic convergence under an Ornstein–Uhlenbeck (OU) process of evolution (Hansen 1997). The algorithm consists of two steps that use a stepwise corrected Akaike Information Criterion (AICc). First in a 'forward' step the programme adds regime shifts until there is no further improvement to the model (which we call  $OU_{NC}$ , non-convergent OU model), then in a 'backward' step the algorithm tries to collapse all pairwise regimes retaining only those that improve the model and therefore finding regimes that are convergent ( $OU_C$ , convergent OU model) (Ingram & Mahler 2013). An advantage of this method is that it is unbiased by *a priori* hypotheses because it does not use any information regarding which taxa belong to particular optima (e.g. it does not use our guild categories). We ran SURFACE on PC1 and PC2 jointly. We compared the fit of this model to a OU model with one phenotypic optimum ( $OU_1$ ), a Brownian motion model (BM) and an OU model with regime shifts that match the ancestral state reconstruction of guild described below ( $OU_{Eco}$ ).

We reconstructed the history of ecological guild evolution using stochastic character mapping, a Bayesian method that samples discrete character state reconstructions under a Markov process of shifts given the species' states and their phylogeny (Huelsenbeck *et al.* 2003). To add uncertainty, we ran 10 000 stochastic character maps to get posterior probabilities for each state at each node (Revell 2014). This was performed with the R package *phytools* (Revell 2012). To visually compare the regimes of phenotypic evolution inferred by SURFACE and the ancestral state reconstruction of guilds, we painted each convergent SURFACE regime with the same colour that was chosen to represent the guild that is most common on that regime. This provides a way to see into the degree of coupling between the phenotypic and ecological evolutionary histories.

### Testing the strength of convergence

With the convergent phenotypic regimes found by SURFACE and the guild information on each species, and because each SURFACE regime had a different most common guild in it, we tested for the strength of convergence on three alternative convergent groupings for each 'ecomorph'. These groupings correspond to (1) 'SURFACE' group: species in the same convergent SURFACE regime, (2) 'Guild' group: species with the same guild (for the arboreal, semi-arboreal, terrestrial and fossorial guilds we performed the measures both excluding species that are obviously not convergent on morphospace and including all of them, see Supplementary Information for further details), and (3) 'SURFACE\*Guild' group: species in the same SURFACE regime that belong to the most common guild on that regime.

The Wheatsheaf index ( $w$ ) is a recently developed method designed to assess the strength of convergence, which in this context is the degree of phenotypic similarity between the species in the convergent group and the dissimilarity of these species from the non-convergent species (Arbuckle *et al.* 2014). To calculate  $w$ , the convergent groups or 'focal' taxa have to be assigned *a priori*. The phenotypic distance between the focal taxa and their phenotypic isolation from the 'non-focal' taxa is then measured, penalising for phylogenetic relatedness. This is achieved using a phenotypic distance matrix ( $d_{ij}$ ), which is corrected for phylogenetic relatedness by dividing the matrix by  $1 - \log(p_{ij} + 0.01)$ , where  $p_{ij}$  is the shared proportional distance of species  $i$  and  $j$  on the tree.  $w$  is then calculated by dividing the mean pairwise phylogenetically corrected distance between all taxa in the study by the mean pairwise distance between the 'focal' taxa only. The larger the mean phenotypic distance between all taxa and the smaller the distance between the 'focal' taxa, the higher the  $w$  index, which equates to stronger convergence (Arbuckle *et al.* 2014). As this is a measure of the strength of convergence, rather than a measure for the presence of convergence, which has to be identified previously, higher  $w$  values simply mean stronger convergence. We calculated the index with the R package *windex* (Arbuckle & Minter 2015). We did not standardise the variables by their standard error because the principal components are on the same scale. For each index, we tested the hypothesis that convergent evolution is significantly stronger than a random distribution of phenotypic values on the same tree topology with 10 000 bootstrap replicates. We calculated  $w$ , its 95% confidence interval by jackknifing the data, and its associated  $P$ -value to make comparisons between these groups.

As a final test for convergence, we calculated five recently developed measures called C1, C2, C3, C4 and C5 to test for convergent evolution (Stayton 2015). Whereas  $w$  measured the phenotypic similarity between the focal taxa and their dissimilarity to the rest of the group, C1–C4 measure the *increase* in similarity between the convergent taxa through evolution, which is useful to distinguish between convergent evolution and stasis. C1 is based on the notion that convergent evolution leads to an increased similarity between descendants compared to the similarity between ancestors. It is measured as  $C1 = 1 - (D_{\text{tip}}/D_{\text{max}})$ , where  $D_{\text{tip}}$  is the distance between the two convergent taxa and  $D_{\text{max}}$  the maximum distance between

any two pair of taxa in those two lineages (extant taxa or ancestors, according to ancestral state reconstruction). Therefore, C1 measures the proportion of phenotypic distance that has been reduced by evolution, and it ranges from 0 to 1, where 1 means they evolved to be identical. The more similar the descendants and the more dissimilar the ancestors, the closer C1 is from 1, and the stronger the convergence. Whereas C1 is a proportion and thus is scaled, C2 measures the magnitude of convergence by measuring the difference between the maximum phenotypic distance between any two taxa (also extant or ancestral) in the lineages and the distance between the convergent taxa, expressed as  $C2 = D_{\text{max}} - D_{\text{tip}}$ . From this, two additional measures can be calculated.  $C3 = C2/L_{\text{tot.clade}}$ , measures the amount of convergent evolution (C2) scaled by the total evolution that has happened in the clade defined by the common ancestor of the convergent taxa and  $C4 = C2/L_{\text{tot.trees}}$ , measures the amount of convergent evolution (C2) scaled by the total evolution in the entire tree (T. Stayton, pers. com.). Put simply, C1 represents the *proportion* of phenotypic distance reduced by convergence between two taxa, C2 the *amount* of convergent evolution between those two taxa, and C3 and C4 the proportion of convergence in the total amount of evolution in the smallest clade containing the convergent taxa and the entire clade respectively. C5 on the other hand is the number of lineages that cross into the region of morphospace defined by the convergent taxa (in other words not the amount or strength but the frequency of convergent evolution). Because the C1–C4 can only be used to compare between two taxa, for each convergent group (as described above for  $w$ ), we performed pairwise comparisons of the convergent lineages by using the two taxa of those lineages that were closest together in morphospace. In addition, for the 'Guild' fossorial convergent group we tested only for the convergence between *Calabaria*, *Anilius* and most *Eryx*, because the convergence between *Cylindrophis* and *Eryx jayakari* is tested in the 'SURFACE' fossorial group. We then averaged the measures for all comparisons for each convergent grouping. To test significance of our measures of C1–C5, we ran 1000 simulations for each comparison using a Brownian Motion model on a variance-covariance matrix based on parameters derived from the data. A  $P$ -value is returned based on the number of times the statistic of the simulation exceeds the observed value to test the hypothesis that convergence is greater than would be expected with no constraints on the direction of evolution. All these measures were calculated with the R package *conevol* (Stayton 2014). In most cases, when the average of the C1–C4 measures was not significant it was due to one or few of the lineages not converging with the others, so examination of the individual comparisons (Table S2) will provide more insight onto where on how strong the convergence is.

## RESULTS

### Evolution and convergence of head shape and phylomorphospace reconstruction

Principal component 1 (PC1) and PC2 accounted for 68.56 and 13.35% of head shape variation respectively. All other

PCs accounted for less than 7% of the variation each, and had no correlation with ecology, and therefore were not considered further. Species group in phylomorphospace according to their ecological guild (Fig. 2). PC1, where more positive values represent a narrowing and elongation of the head (Figs. 2 and S2), separates the fossorial and semi-fossorial species from the arboreal, semi-arboreal, terrestrial and semi-aquatic species. This demonstrates that burrowing species have broader and shorter heads with smaller eyes, whereas the other guilds have thinner heads and longer heads with larger eyes. PC2, where more positive values represent a lateralisation of the eyes and nostrils, a broadening and shortening of the back of the mouth and a sharpening of the snout (i.e. a more 'funnel-shaped' head), separates the non-burrowing guilds from positive to negative values in the following order: arboreal, semi-arboreal, terrestrial and semi-aquatic. This implies that semi-aquatic species, and to a lesser degree terrestrial species,

have a more 'streamlined' head shape with more dorsally placed eyes and nostrils, and that this shape progressively turns into a funnel-shape with lateral eyes and nostrils towards the arboreal region of phylomorphospace. The fossorial species on the other hand occupy the same PC2 phylomorphospace as the non-burrowers, ranging from the pointy-headed *Rhinophis* to the broad and round-headed *Eryx jayakari* and *Cylindrophis*, whereas the semi-fossorial species display narrow variation in PC2 in the middle of the morphospace.

### Phenotypic convergent regimes and ancestral state reconstruction

The SURFACE analysis, which looks for convergent regimes of evolution on the phylogeny, found eight distinct phenotypic regimes of evolution (Figs. 2 and 3). Five of these are convergent and were reached independently multiple times. Twelve

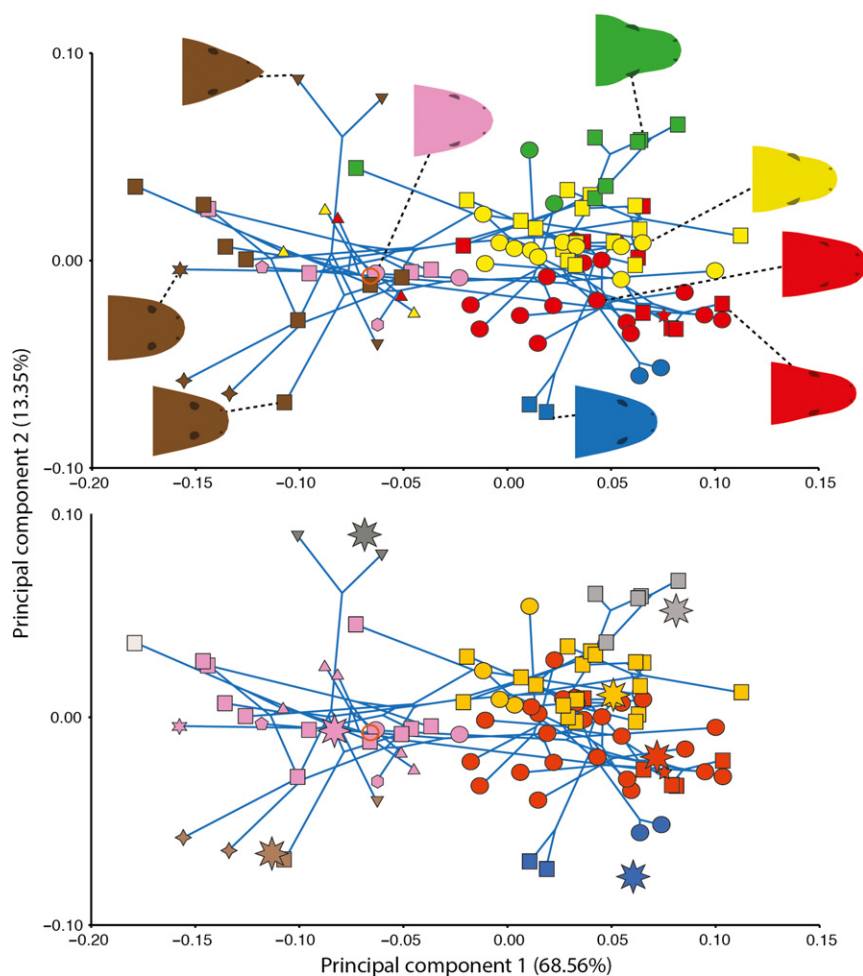


**Figure 2** Phylomorphospace of head shape in pythons and boas. Principal component analysis on species average for head shape based on geometric morphometrics of 35 landmarks and semi-landmarks, with the molecular phylogeny mapped onto the morphospace and internal nodes reconstructed with squared-change parsimony. Above, species coloured by ecological guild. Below, species coloured by SURFACE phenotypic regime. Colours correspond to guild or most common guild in SURFACE regime as follows: green, arboreal; yellow, semi-arboreal; red, terrestrial; blue, semi-aquatic; pink, semi-fossorial; brown, fossorial. Shapes correspond to taxonomic categories as follows: circles, Pythonidae; squares, Booidea; triangles, Tropidophiidae; pentagon, Loxocemidae; hexagon, Xenopeltidae; four-point star, Cylindrophiiidae; inversed triangle, Uropletiidae; six-point star, Aniliidae; five-point star, Bolyeriidae. The orange ring corresponds to the reconstructed root node of the tree. Below: large eight-pointed stars correspond to adaptive optimums ( $\theta$ ) for the regimes found by SURFACE.

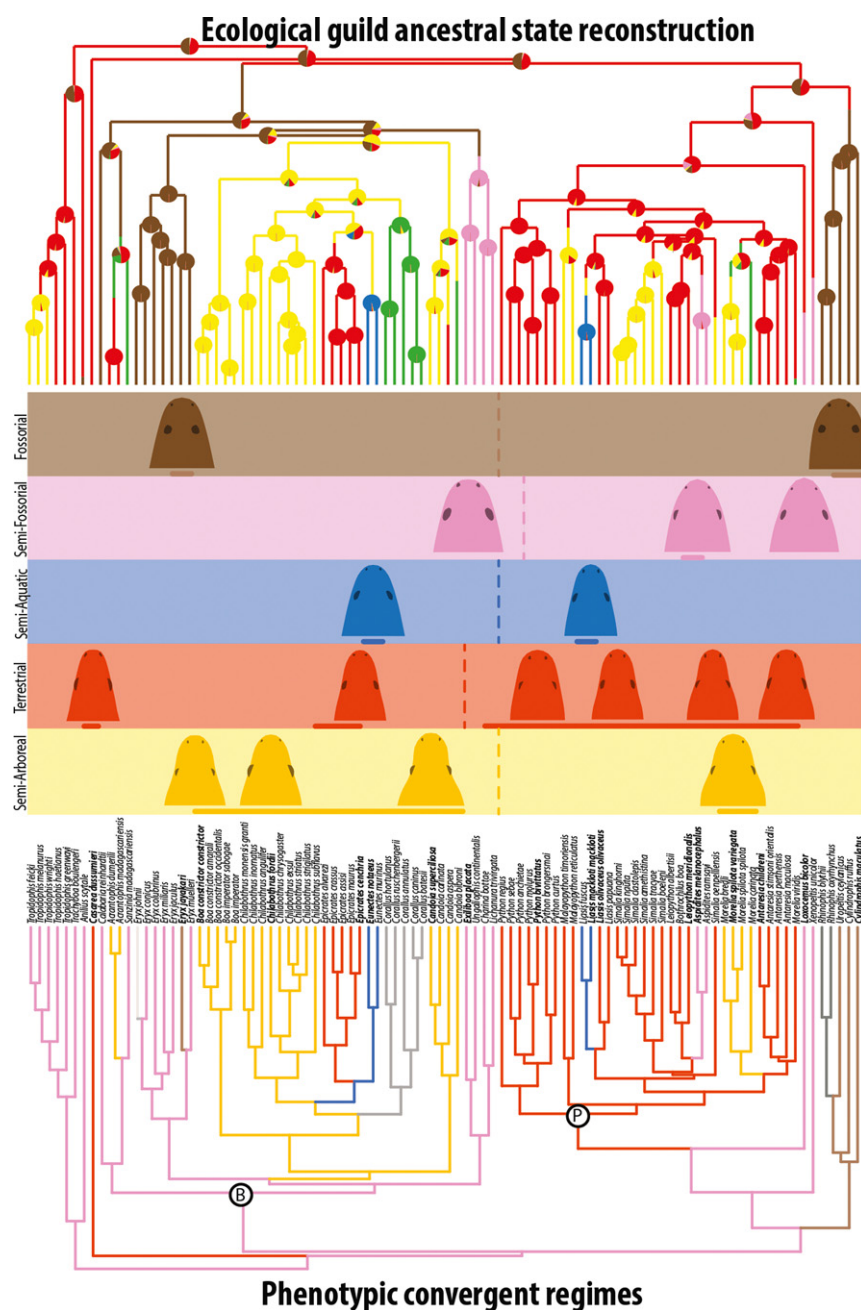


**Figure 3** Phenotypic convergent regimes and guild ancestral state reconstruction. Above, an ancestral state reconstruction of guild on the henophidian phylogeny. Branch colours correspond to guilds as in the legend in Fig. 2. Pie charts on nodes illustrate posterior probabilities for each state. Below, the SURFACE analysis results on the phylogeny. Grey scale regimes are not convergent, whereas all coloured ones are convergent. Each SURFACE regime is coloured according to the predominant guild on that regime. This figure demonstrates the strong relationship between the convergent phenotypes and their guild based on two independent data sets. Coloured columns between the two trees display examples of convergent ecomorphs found by matching same-coloured tips between the SURFACE and guild trees. Species names used as examples are in bold. The coloured bars below the heads are to indicate where on the phylogeny that regime is located.

of the 15 regime *shifts* are towards convergent regimes, giving a convergence fraction of 0.8 (Table 1). The best model found by the 'backward' step with convergent regimes ( $OU_C$ ;  $AIC_c = -813.48$ ) showed an improvement over all the other models ( $OU_{NC}$ ,  $\Delta AIC_c = 26.24$ ;  $OU_1$ ,  $\Delta AIC_c = 103.06$ ;  $OU_{Eco}$ ,  $\Delta AIC_c = 110.57$ ;  $BM$ ,  $\Delta AIC_c = 88.38$ ) (see Fig. S3 and Table 1). For the  $OU_C$  model, the trait specific rate of adaptation,  $\alpha$  for PC1 and PC2 is 5.796 and 9.563 million years<sup>-1</sup>

respectively. Converted to phylogenetic half-life ( $t_{1/2}$ ), which translates into half the time required for a lineage to reach an adaptive optimum, these correspond to 0.12 and 0.073 My (Table 1). The species phenotypes tend to cluster around the estimated adaptive optima ( $\theta$ ), which makes the model a realistic representation of morphological evolution (Fig. 2). See Table 1 for the parameters for all the models fitted.



**Table 1** Convergence parameters found by the SURFACE analysis on phenotypic convergent evolution in boas and pythons. Parameters were found by the evolutionary models fitted to the evolution of head morphology in pythons and boas described by PC1 and PC2. OU<sub>C</sub>: multi peaked convergent OU model fitted by the backward phase of SURFACE. OU<sub>NC</sub>: multi peaked non-convergent OU model fitted by the forward phase of SURFACE. OU<sub>Eco</sub>: multi peaked OU model based on the stochastic character mapping of guilds. OU1: single peak OU model. BM: Brownian motion model.  $\theta_{arboreal(a)}$  corresponds to the  $\theta$  parameter for the arboreal regime for OU<sub>C</sub> and OU<sub>Eco</sub> models but for the only regime in the OU1 model

Parameter	OU <sub>C</sub>		OU <sub>NC</sub>		OU <sub>Eco</sub>		OU1		BM	
AICc	−813.14		−786.9		−702.57		−710.08		−724.76	
Phenotypic regimes	8		15		7		1		–	
Phen. reg. shifts (a)	15		15		26		1		–	
Conv. phen. regimes	5		–		6		–		–	
Conv. reg. shifts (b)	12		–		26		–		–	
Conv. fraction (b/a)	0.8		–		1		–		–	
	PC1	PC2	PC1	PC2	PC1	PC2	PC1	PC2	PC1	PC2
$\alpha$	5.796	9.563	10.929	8.955	4.121	2.377	0.191	0.501	–	–
$t_{1/2}$	0.12	0.073	0.063	0.077	0.168	0.292	3.629	1.384	–	–
$\sigma^2$	0.013	0.005	0.019	0.004	0.013	0.003	0.009	0.003	0.009	0.003
$\theta_{arboreal(a)}$	–	–	–	–	0.037	0.103	−0.049	−0.004	–	–
$\theta_{semi-arboreal}$	0.046	0.017	–	–	0.036	0.029	–	–	–	–
$\theta_{terrestrial}$	0.067	−0.013	–	–	0.06	−0.024	–	–	–	–
$\theta_{semi-aquatic}$	0.055	−0.071	–	–	0.043	−0.138	–	–	–	–
$\theta_{semi-fossorial}$	−0.089	$-3 \times 10^{-4}$	–	–	−0.102	$4 \times 10^{-5}$	–	–	–	–
$\theta_{fossorial}$	−0.119	−0.06	–	–	−0.122	−0.004	–	–	–	–

The stochastic character mapping (ancestral state reconstruction) of guild on the phylogeny reconstructed the terrestrial and fossorial guilds as the most likely in the common ancestor of all henophidians (Fig. 3). Each phenotypic regime identified on SURFACE had a different most common guild among the species in it. After each SURFACE regime was coloured according to the predominant guild in that regime, and subsequently compared to the guild ancestral state reconstruction tree, 54 of the 94 taxa of all henophidians and 51 of the 79 pythons and boas had the same colour in both trees, illustrating the degree of coupling between phenotypic and ecological variation (Fig. 3).

### Strength of convergence

We used  $w$  and the C1–C5 measures to test for the strength of convergence in the identified convergent ‘ecomorphs’ or guild-phenotype associations. For each guild category we applied these measures to three alternative ecomorph groupings: (1) by shared SURFACE regime, (2) by shared guild, and (3) species in each SURFACE regime that belong to the most common guild on that regime (to which we refer as SURFACE\*Guild). While SURFACE did not find a convergent regime corresponding to the arboreal species,  $w$  and C1–C4 for the arboreal ecomorph, which are statistically significant and have a very narrow CI for  $w$ , indicate that they show a similar degree of convergence to the other ecomorphs (Tables 2 and 3). C1 measures an average phenotypic distance closed by convergence between the arboreal clades of 83.2%. All three alternative groupings of semi-arboreal and terrestrial ecomorphs have highly significant  $P$ -values and very narrow CIs associated to their  $w$  (Table 2). Moreover, C1 indicates convergence ranging from 67.5% to 97.1% between lineages of semi-arboreal or terrestrial ecomorphs. The semi-aquatic ecomorph, which includes the anaconda boas and the water pythons, had the highest  $w$  index (see Table 2 and Fig. S4)

because they are the most phenotypically isolated ecomorph and therefore also have the only statistically significant measure of C5. However, C1 was not significant for this guild (Table 3). Since SURFACE identified a convergent regime only including all of the four semi-aquatic species, the three ecomorph alternatives are identical in this case. Between the semi-fossorial grouping alternatives the highest and only significant  $w$  and C1 is obtained by the ‘SURFACE’ grouping, which indicates that 98.1% of the similarity between the two convergent lineages found by SURFACE has evolved by convergent evolution (Tables 2 and 3). For the fossorial grouping alternatives,  $w$  is not significant, but for the ‘SURFACE’ and ‘SURFACE\*Guild’ (which are the same in this case since all the species found in this SURFACE regime are fossorial)  $w$  is high compared to the values of the other ecomorphs (Table 2). On the other hand, C1 is high and significant for the fossorials, indicating that convergence has at least closed in average 77% in of the distance between fossorial lineages (Table 3).

It is clear that a multi peaked OU model with multiple and abrupt shifts is a better fit for head shape evolution in henophidian snakes. C indices, which are calculated assuming Brownian motion, in this case when the data better fits an adaptive model, will tend to under-estimate convergence, therefore the results indicating strong convergence by this index are robust.

### DISCUSSION

We found compelling evidence that pythons and boas are remarkable examples of replicated adaptive radiations where parallel adaptation to similar life-styles has resulted in the independent evolution of similar phenotypes. Convergent ecomorphs were supported by multiple analytical techniques in each of the six ecological guilds. Distantly related species that share the same ecology also occupy the same morphospace, providing strong evidence for adaptive convergence.

**Table 2** Wheatsheaf index ( $w$ ). For the three alternative convergent ecomorph groupings for each guild. The groupings are according to (1) 'SURFACE': species on the same SURFACE regime, (2) 'Guild (convergent)': species with the same ecological guild category excluding the few taxa that are obviously non-convergent with the rest of the guild, (3) 'Guild (all)': species with the same ecological guild category, not excluding the obviously non-convergent taxa (4) 'SURFACE\*Guild': species on a SURFACE regime that belong to the most common guild on that regime.  $P$ -values are derived from the hypothesis that convergent evolution is significantly stronger than a random distribution of phenotypic values based 10 000 bootstrap replicates, and 95% CI on a jackknife of the data.

Convergent regimes	Arboreal	Semi-Arboreal	Terrestrial	Semi-Aquatic	Semi-Fossorial	Fossorial
SURFACE	–	1.72 ( $P \sim 0$ )	1.34 ( $P \sim 0$ )	3.84 ( $P = 0.0161$ )	1.93 ( $P = 0.0015$ )	1.96 ( $P = 0.1854$ )
Guild (convergent)	2.43 ( $P = 0.012$ )	1.86 ( $P \sim 0$ )	1.52 ( $P = 0.0004$ )	3.84 ( $P = 0.0161$ )	1.64 ( $P = 0.0565$ )	1.25 ( $P = 0.1354$ )
Guild (all)	1.62 ( $P = 0.0189$ )	1.76 ( $P \sim 0$ )	1.52 ( $P = 0.0005$ )	3.84 ( $P = 0.0161$ )	1.64 ( $P = 0.0565$ )	1.1 ( $P = 0.3162$ )
SURFACE*Guild	–	1.71 ( $P \sim 0$ )	1.47 ( $P = 0.0003$ )	3.84 ( $P = 0.0161$ )	1.64 ( $P = 0.0565$ )	1.96 ( $P = 0.1854$ )
95% Confidence Intervals						
SURFACE	–	1.69–1.79	1.31–1.39	3.19–3.84	1.89–1.97	1.92–2.05
Guild (convergent)	2.4–2.52	1.83–1.94	1.49–1.58	3.19–3.84	1.6–1.71	1.19–1.32
Guild (all)	1.58–1.63	1.74–1.83	1.49–1.57	3.19–3.84	1.6–1.71	1.07–1.14
SURFACE*Guild	–	1.67–1.75	1.42–1.54	3.19–3.84	1.6–1.71	1.92–2.05

Values in bold are statistically significant ( $P < 0.05$ ).

**Table 3** C1–C5 convergence measures and  $P$ -values.  $P$ -values were derived from 1000 simulations to test the hypothesis that the observed values are greater than random simulations based on Brownian motion. For each alternative convergent grouping according to the three different grouping criteria (as in Table 2). Groupings with the same superscript number have equal C1–C4 values because they include the same lineages. Values in bold are statistically significant ( $P < 0.05$ ).

Convergent group	C1	C2	C3	C4	C5
SURFACE Semi-Arboreal	0.791 ( $P = 0.065$ )	0.084 ( $P = 0.032$ )	0.032 ( $P = 0.065$ )	0.021 ( $P = 0.063$ )	11 ( $P = 0.21$ )
SURFACE Terrestrial <sup>1</sup>	0.938 ( $P = 0.002$ )	0.129 ( $P = 0$ )	0.035 ( $P = 0.002$ )	0.032 ( $P = 0.001$ )	5 ( $P = 0.649$ )
SURFACE Semi-Aquatic <sup>2</sup>	0.623 ( $P = 0.111$ )	0.08 ( $P = 0.039$ )	0.022 ( $P = 0.086$ )	0.02 ( $P = 0.084$ )	4 ( $P = 0.017$ )
SURFACE Semi-Fossorial	0.983 ( $P = 0$ )	0.106 ( $P = 0.003$ )	0.026 ( $P = 0.015$ )	0.026 ( $P = 0.015$ )	4 ( $P = 0.851$ )
SURFACE Fossorial <sup>3</sup>	0.773 ( $P = 0.034$ )	0.093 ( $P = 0.015$ )	0.026 ( $P = 0.031$ )	0.023 ( $P = 0.027$ )	4 ( $P = 0.099$ )
Guild Arboreal (convergent)	0.832 ( $P = 0.02$ )	0.084 ( $P = 0.012$ )	0.044 ( $P = 0.036$ )	0.021 ( $P = 0.039$ )	7 ( $P = 0.143$ )
Guild Arboreal (all)	0.47 ( $P = 0.35$ )	0.05 ( $P = 0.32$ )	0.02 ( $P = 0.35$ )	0.01 ( $P = 0.35$ )	9 ( $P = 0.245$ )
Guild Semi-Arboreal (convergent)	0.84 ( $P = 0.018$ )	0.06 ( $P = 0.078$ )	0.027 ( $P = 0.129$ )	0.015 ( $P = 0.121$ )	6 ( $P = 0.675$ )
Guild Semi-Arboreal (all)	0.47 ( $P = 0.35$ )	0.05 ( $P = 0.32$ )	0.02 ( $P = 0.35$ )	0.01 ( $P = 0.35$ )	4 ( $P = 0.587$ )
Guild Terrestrial (convergent)	0.675 ( $P = 0.111$ )	0.083 ( $P = 0.083$ )	0.029 ( $P = 0.109$ )	0.021 ( $P = 0.114$ )	5 ( $P = 0.662$ )
Guild Terrestrial (all)	0.59 ( $P = 0.16$ )	0.073 ( $P = 0.12$ )	0.024 ( $P = 0.162$ )	0.018 ( $P = 0.165$ )	3 ( $P = 0.639$ )
Guild Semi-Aquatic <sup>2</sup>	0.623 ( $P = 0.111$ )	0.08 ( $P = 0.039$ )	0.022 ( $P = 0.086$ )	0.02 ( $P = 0.084$ )	4 ( $P = 0.017$ )
Guild Semi-Fossorial <sup>4</sup>	0.593 ( $P = 0.1$ )	0.06 ( $P = 0.095$ )	0.034 ( $P = 0.116$ )	0.015 ( $P = 0.119$ )	8 ( $P = 0.514$ )
Guild Fossorial (convergent)	0.799 ( $P = 0.023$ )	0.088 ( $P = 0.01$ )	0.03 ( $P = 0.027$ )	0.022 ( $P = 0.026$ )	6 ( $P = 0.616$ )
Guild Fossorial (all)	0.51 ( $P = 0.21$ )	0.057 ( $P = 0.19$ )	0.019 ( $P = 0.23$ )	0.014 ( $P = 0.23$ )	4 ( $P = 0.879$ )
SURFACE*Guild Semi-Arboreal	0.889 ( $P = 0.007$ )	0.084 ( $P = 0.023$ )	0.024 ( $P = 0.061$ )	0.021 ( $P = 0.057$ )	11 ( $P = 0.209$ )
SURFACE*Guild Terrestrial <sup>1</sup>	0.938 ( $P = 0.002$ )	0.129 ( $P = 0$ )	0.035 ( $P = 0.002$ )	0.032 ( $P = 0.001$ )	5 ( $P = 0.649$ )

Furthermore, a similar pattern of evolutionary shifts through the phylogeny is observed in both SURFACE and the ancestral state reconstruction of ecology (Fig. 3). This suggests a tight coupling between adaptation to different ecological lifestyles and phenotypic evolution, and therefore a strong adaptive component to head shape diversity.

One of the best known cases of convergent evolution in the animal world is that of the arboreal green tree python (*Morelia viridis* (Schlegel, 1872)) and the emerald tree boa [*Corallus caninus* (Linnaeus, 1758)] where both exhibit the same arboreal perching behaviour, overall appearance (Fig. 1) and ontogenetic colour change. Here, we have shown that pythons and boas exhibit convergence in every guild, and also are convergent with other related clades including the Asian pipe snakes (Cylindrophidae) and the critically endangered bolyeriid *Casarea dussumieri* (Schlegel, 1837). In pythons and boas most convergence happens within the terrestrial and semi-arboreal ecomorphs, which are the most common micro-habitats. Semi-

arboreal boas in Central and South America and Melanesia have converged in head shape with several pythons in south-east Asia and Australo-Papua. Similarly, the terrestrial rainbow boas in South America have evolved similar head phenotypes to terrestrial pythons in the Old World. In contrast, similarity between the non-python semi-fossorial species (Loxocemidae, Xenopeltidae and Charinidae), might not be convergence but simply shared ancestral states (Fig. 3). This pattern could be driven by evolutionary stasis (Burt 2001; Muschick *et al.* 2012), and is the same reason why sharks and teleost fishes, and lizards and salamanders have similar body plans despite being only distantly related. Fossorial snakes encompass as much morphological diversity as the arboreal, semi-arboreal, terrestrial and semi-aquatic snakes put together. There are many different ways a snake can be a 'burrower'. We found that they have wider and shorter snouts than the other ecomorphs, but they range from the arrow-headed with laterally placed eyes *Rhinophis* to the round headed with



dorsally placed eyes *Eryx jayakari* and *Cylindrophis*. These differences may reflect adaptations to different burrowing methods (drilling vs. shovelling) and/or substrates (mud vs. sand).

Snake phenotypes are constrained because they are limbless, gape-limited and swallow their prey whole, therefore the number of morphologies they can evolve to respond to particular selective pressures is probably limited, which promotes convergence between snakes (Fabre *et al.* 2016). Because the main phenotypic differences among guilds are the placement of the eyes and the outline of the head (e.g. more dorsally placed eyes and streamlined heads in semi-aquatic and to a lesser degree terrestrial species) our results suggest that vision in relation to habitat use and movement through the micro-habitat are important functional constraints on morphology in henophidians. Perhaps the best comparison to the python/boa system is the morphological convergence between North American colubroid and Australian elapid snakes (Grundler & Rabosky 2014). Like pythons and boas, their convergence is clade-wide, intercontinental and driven by adaptation to habitat use. Their study and ours supports the hypothesis that micro-habitat use is the key driver of morphological diversity in snakes.

Convergent morphological evolution in vertebrates has been demonstrated in a number of groups such as Great Lake African cichlid fishes and Caribbean anole lizards (Muschick *et al.* 2012; Mahler *et al.* 2013). These well-studied systems have several features in common – they all occur between isolated but geographically close islands (or lakes), they are relatively closely related (single genus or family) with a divergence at least in the Cenozoic, and the phenotypic and ecological differences are sometimes subtle. Convergent evolution at deeper levels of the vertebrate phylogeny has been studied in a quantitative and/or phylogenetic context (Bossuyt & Milinkovitch 2000; Donley *et al.* 2004; Melville *et al.* 2006; Grundler & Rabosky 2014; Moen *et al.* 2015), however, intercontinental and distantly related replicated adaptive radiations are rare and theoretically unexpected (Losos 2010). Landmark examples of convergent evolution between vertebrates, such as birds, bats and pterosaurs, or sharks, dolphins and ichthyosaurs are undeniably convergent in functional morphology and body plan, but analytical techniques to quantify strength and frequency of convergence have not been applied to these groups. A species-by-species matching and a potential case of convergence between adaptive radiations has been proposed for eutherian and placental mammals (Futuyma 1998). Independent origins of morphotypes such as ‘wolves’, ‘anteaters’, ‘mice’ and ‘moles’ in these two radiations are remarkable but they are not part of ‘replicated radiations’. The convergence between pythons and boas adds to a recent body of evidence demonstrating that evolution can still be predictable at deeper time-scales (Moen *et al.* 2015). Finding such strong and constant ecomorphological associations can help us, e.g. predict the ecological niche of extinct species based on their morphology.

Deep and clade-wide convergence appears then to be very rare, but further application of emerging analytical techniques to apparently similar groups (e.g. penguins and auks) may reveal a wider phenomenon in evolutionary biology. Our study demonstrates the utility of recently developed methods to detect and quantify convergent evolution. SURFACE, without any *a priori* information on which taxa might be

convergent, efficiently finds phenotypic regimes that have been discovered independently in different lineages (Ingram & Mahler 2013; Mahler *et al.* 2013; Ingram & Kai 2014). *w* and the *C* indices, which measure the strength of or degree of suspected convergence, provide additional metrics for the convergent regimes found by SURFACE and for the regimes defined by ecology only, and provide a useful comparison between these two.

Convergent evolution is not always driven by natural selection – it also can be caused by genetic, functional or developmental constraints that limit the number of phenotypes an organism can evolve (Wake 1991; Brakefield 2006) and can even arise by chance (Stayton 2008). We have demonstrated that the strong selective pressures related to habitat-use have driven the remarkable and ubiquitous ecomorphological convergent evolution among pythons, boas and their relatives, and we speculate that common constraints on how head shape can adapt also contribute to this repeated evolution of the same morphologies. Moreover, they provide a new model adaptive radiation system for the study of macro-evolutionary patterns of morphological evolution, at a deeper divergence level than the established adaptive radiation models.

## ACKNOWLEDGEMENTS

We thank the museum curators and curatorial assistants for the help during our data collecting, Graham Reynolds for providing us with the phylogeny, the photographers who kindly allowed us to use their photographs for Fig. 1 (credits on figure legend), Iliana Medina for providing helpful comments and insights into the analyses and main figures, Tristan Stayton for help with his *convevol* package, Jonathan Losos, Michael Jennions, Mitzy Pepper, Ian Brennan, Emma Sherratt and three anonymous reviewers for helpful comments that greatly improved the paper and Peter Tolson for providing us information on the natural history of West Indian boas. We finally thank the ACT Herpetological Association, the Peter Ranking Trust Fund for Herpetology, the American Museum of Natural History, the Australian National University and the Australian Research Council for funding this project. DE is supported by a Becas Chile – CONICYT scholarship.

## AUTHORSHIP

Both authors conceived and planned the project and wrote the manuscript. D.E. collected and analysed the data and prepared the figures.

## REFERENCES

- Arbuckle, K. & Minter, A. (2015). Windex: analyzing convergent evolution using the WheatSheaf index in R. *Evol. Bioinform.*, 11, 11–14.
- Arbuckle, K., Bennett, C.M. & Speed, M.P. (2014). A simple measure of the strength of convergent evolution. *Methods Ecol. Evol.*, 5, 685–693.
- Arendt, J. & Reznick, D. (2008). Convergence and parallelism reconsidered: what have we learned about the genetics of adaptation?. *Trends Ecol. Evol.*, 23, 26–32.
- Bossuyt, F. & Milinkovitch, M.C. (2000). Convergent adaptive radiations in Madagascan and Asian ranid frogs reveal covariation between larval and adult traits. *Proc. Natl Acad. Sci. USA*, 97, 6585–6590.

- Brakefield, P.M. (2006). Evo-devo and constraints on selection. *Trends Ecol. Evol.*, 21, 362–368.
- Burt, D.B. (2001). Evolutionary stasis, constraint and other terminology describing evolutionary patterns. *Biol. J. Linnean Soc.*, 72, 509–517.
- Donley, J.M., Sepulveda, C.A., Konstantinidis, P., Gemballa, S. & Shadwick, R.E. (2004). Convergent evolution in mechanical design of lamnid sharks and tunas. *Nature*, 429, 61–65.
- Fabre, A.C., Bickford, D., Segall, M. & Herrel, A. (2016). The impact of diet, habitat use, and behaviour on head shape evolution in homalopsid snakes. *Biol. J. Linnean Soc.*, in press.
- Futuyma, D.J. (1998). *Evolutionary Biology*, 3rd edn. Sinauer Associates, Sunderland, MA.
- Gavrilits, S. & Losos, J.B. (2009). Adaptive radiation: contrasting theory with data. *Science*, 323, 732–737.
- Grundler, M.C. & Rabosky, D.L. (2014). Trophic divergence despite morphological convergence in a continental radiation of snakes. *Proc. R. Soc. B*, 281, 20140413.
- Hansen, T.F. (1997). Stabilizing selection and the comparative analysis of adaptation. *Evolution*, 51, 1341–1351.
- Harmon, L.J., Kolbe, J.J., Cheverud, J.M. & Losos, J.B. (2005). Convergence and the multidimensional niche. *Evolution*, 59, 409–421.
- Harvey, P.H. & Pagel, M.D. (1991). *The Comparative Method in Evolutionary Biology*. Oxford University Press, Oxford, UK.
- Hsiang, A.Y., Field, D.J., Webster, T.H., Behlke, A.D., Davis, M.B., Racicot, R.A. *et al.* (2015). The origin of snakes: revealing the ecology, behavior, and evolutionary history of early snakes using genomics, phenomics, and the fossil record. *BMC Evol. Biol.*, 15, 1–22.
- Huelsenbeck, J.P., Nielsen, R. & Bollback, J.P. (2003). Stochastic mapping of morphological characters. *Syst. Biol.*, 52, 131–158.
- Ingram, T. & Kai, Y. (2014). The geography of morphological convergence in the radiations of pacific *Sebastes* rockfishes. *Am. Nat.*, 184, E115–E131.
- Ingram, T. & Mahler, D.L. (2013). SURFACE: detecting convergent evolution from comparative data by fitting Ornstein-Uhlenbeck models with stepwise Akaike Information Criterion. *Methods Ecol. Evol.*, 4, 416–425.
- Klingenberg, C.P. (2011). MorphoJ: an integrated software package for geometric morphometrics. *Mol. Ecol. Resour.*, 11, 353–357.
- Klingenberg, C.P. & Gidaszewski, N.A. (2010). Testing and quantifying phylogenetic signals and homoplasy in morphometric data. *Syst. Biol.*, 59, 245–261.
- Klingenberg, C.P., Barluenga, M. & Meyer, A. (2002). Shape analysis of symmetric structures: quantifying variation among individuals and asymmetry. *Evolution*, 56, 1909–1920.
- Losos, J.B. (2010). Adaptive radiation, ecological opportunity, and evolutionary determinism. *Am. Nat.*, 175, 623–639.
- Losos, J.B. (2011). Convergence, adaptation, and constraint. *Evolution*, 65, 1827–1840.
- Maddison, W.P. (1991). Squared-change parsimony reconstructions of ancestral states for continuous-valued characters on a phylogenetic tree. *Syst. Zool.*, 40, 304–314.
- Mahler, D.L. & Ingram, T. (2014). Phylogenetic comparative methods for studying clade-wide convergence. In: *Modern Phylogenetic Comparative Methods and their Application in Evolutionary Biology*. (ed Garamszegi, L.Z.). Springer, Berlin Heidelberg, Berlin, Heidelberg, pp. 425–450.
- Mahler, D.L., Ingram, T., Revell, L.J. & Losos, J.B. (2013). Exceptional convergence on the macroevolutionary landscape in island lizard radiations. *Science*, 341, 292–295.
- McGhee, G. (2011). *Convergent Evolution: Limited Forms Most Beautiful*. Massachusetts Institute of Technology, Cambridge, MA.
- Melville, J., Harmon, L.J. & Losos, J.B. (2006). Intercontinental community convergence of ecology and morphology in desert lizards. *Proc. R. Soc. B*, 273, 557–563.
- Moen, D.S., Morlon, H. & Wiens, J.J. (2015). Testing convergence versus history: convergence dominates phenotypic evolution for over 150 million years in frogs. *Syst. Biol.*, 65, 146–160.
- Muschick, M., Indermaur, A. & Salzburger, W. (2012). Convergent evolution within an adaptive radiation of cichlid fishes. *Curr. Biol.*, 22, 2362–2368.
- Paradis, E., Claude, J. & Strimmer, K. (2004). APE: analyses of phylogenetics and evolution in R language. *Bioinformatics*, 20, 289–290.
- Pyron, R.A. & Burbrink, F.T. (2014). Early origin of viviparity and multiple reversions to oviparity in squamate reptiles. *Ecol. Lett.*, 17, 13–21.
- R Development Core Team. (2015). *R: A Language and Environment for Statistical Computing* [Online]. Vienna, Austria: R Foundation for Statistical Computing. Available at: <http://www.R-project.org>. Last accessed 11 November 2014.
- Revell, L.J. (2012). Phytools: an R package for phylogenetic comparative biology (and other things). *Methods Ecol. Evol.*, 3, 217–223.
- Revell, L.J. (2014). Graphical methods for visualizing comparative data on phylogenies. In: *Modern Phylogenetic Comparative Methods and Their Application in Evolutionary Biology*. (ed Garamszegi, L.Z.). Springer, Berlin Heidelberg, Berlin, Heidelberg, pp. 77–103.
- Reynolds, G.R., Niemiller, M.L. & Revell, L.J. (2014). Toward a tree-of-life for the boas and pythons: multilocus species-level phylogeny with unprecedented taxon sampling. *Mol. Phylogenet. Evol.*, 71, 201–213.
- Rohlf, F.J. (2015). The tps series of software. *Hystrix*, 26, 1–4.
- Rohlf, F.J. & Slice, D. (1990). Extensions of the Procrustes method for the optimal superimposition of landmarks. *Syst. Biol.*, 39, 40–59.
- Schluter, D. (2000). *The Ecology of Adaptive Radiation*. Oxford University Press, Oxford, UK.
- Sidlauskas, B. (2008). Continuous and arrested morphological diversification in sister clades or characiform fishes: a phylomorphospace approach. *Evolution*, 62, 3135–3156.
- Simpson, G.G. (1953). *The Major Features of Evolution*. Columbia University Press, New York, NY.
- Stayton, C.T. (2008). Is convergence surprising? An examination of the frequency of convergence in simulated datasets. *J. Theor. Biol.*, 252, 1–14.
- Stayton, C.T. (2014). Convevol: Quantifies and Assesses the Significance of Convergent Evolution. R package version 1.0. Available at: <http://cran.r-project.org/web/packages/convevol/index.html>. (Last accessed 10 October 2015)
- Stayton, C.T. (2015). The definition, recognition, and interpretation of convergent evolution, and two new measures for quantifying and assessing the significance of convergence. *Evolution*, 69, 2140–2153.
- Streicher, J.W. & Wiens, J.J. (2016). Phylogenomic analyses reveal novel relationships among snake families. *Mol. Phylogenet. Evol.*, 100, 160–169.
- Uyeda, J.C., Caetano, D.S. & Pennell, M.W. (2015). Comparative analysis of principal components can be misleading. *Syst. Biol.*, 64, 677–689.
- Wainwright, P.C., Alfaro, M.E., Bolnick, D.I. & Hulse, C.D. (2005). Many-to-one mapping of form to function: a general principle in organismal design? *Integr. Comp. Biol.*, 45, 256–262.
- Wake, D.B. (1991). Homoplasy: the result of natural selection, or evidence of design limitations? *Am. Nat.*, 138, 543–567.
- Zelditch, M.L., Swiderski, D.L. & Sheets, H.D. (2012). *Geometric Morphometrics for Biologists: A Primer*, 2nd edn. Academic Press, London, UK.
- Zheng, Y. & Wiens, J.J. (2016). Combining phylogenomic and supermatrix approaches, and a time-calibrated phylogeny for squamate reptiles (lizards and snakes) based on 52 genes and 4162 species. *Mol. Phylogenet. Evol.*, 94, 537–547.

## SUPPORTING INFORMATION

Additional Supporting Information may be found online in the supporting information tab for this article.

Editor, Luke Harmon

Manuscript received 1 March 2016

First decision made 11 April 2016

Manuscript accepted 26 April 2016